Optical gain and threshold current density of strained wurtzite GaN/AlGaN quantum dot lasers

H. Bouchenafa[a,b,*], and B. Benichou[c]

[a] *Department of Physics, Faculty of Exact Sciences and Informatics, Hassiba Benbouali University of Chlef, 02000 Chlef, Algeria.*
**e-mail: bouchenafa_halima@yahoo.fr*
[b] *Laboratory for Theoretical Physics and Material Physics, Hassiba Benbouali University, Chlef 02000, Algeria.*
[c] *Department of Electronics, Faculty of Technology, Hassiba Benbouali University of Chlef, Chlef 02000, Algeria.*

Received 16 April 2022; accepted 13 June 2022

In this work, the influences of biaxial compressive and tensile strains on optical gain and threshold current density are investigated theoretically as a function of the side lengths of the quantum box in the GaN/$Al_{0.2}Ga_{0.8}N$ structure by using a model based on the density matrix theory of semiconductor lasers with relaxation broadening. For various side lengths of the quantum box, we compare the spectra gain curves of compressive, tensile-strained, and unstrained structures of the GaN/$Al_{0.2}Ga_{0.8}N$ cubic quantum-dot (QD) laser. The dependence of peak optical gain on carrier density and the modal gain on current density is plotted too for all cases. The results reveal that many enhancements can be made to the laser structure by introducing -0.5% compressive strain: a higher value of optical gain of 18421 cm^{-1} at $L = 60$ Å, a lower value of transparency of carrier density of $N_{tr} = 0.13 \times 10^{19}$ cm^{-3} and transparency current density of $J_{tr} = 26.9$ A/cm^2 and a lower threshold current density of $J_{th} = 78.87$ A/cm^2 at $L = 100$ Å.

Keywords: Quantum dot lasers; optical gain; III-N semiconductors; biaxial strain; threshold current density.

DOI: https://doi.org/10.31349/RevMexFis.69.010503

1. Introduction

Modern opto-electronic devices, such as laser diodes (LDs) and light-emitting diodes (LEDs), rely heavily on semiconductor nanostructures (LEDs). The benefits of utilizing quantum dots in the active region of these devices stem from the three-dimensional confinement of charge carriers, which results in a delta function-like density of states [1–4]. In order to achieve the target wavelengths of multiple applications in entertainment technologies, telecommunications, and medical engineering, various material systems must be used for the active regions.

Especially for optoelectronics, group III-nitride compounds and alloys have emerged as an essential and versatile class of semi-conductor materials. Although GaN, AlN, and InN all crystallize in the wurtzite structure [5], their band gaps are substantially different, ranging from 0.7 eV for InN to 6.2 eV for AlN [6]. At room temperature, ternary alloys with a wide bandgap range of 0.7 to 6.2 eV can be created by combining Indium and Aluminum with GaN, covering the spectral range from deep ultraviolet (UV) to infrared (IR) [7, 8].

Strain is always present in group III-nitride based devices due to the significant differences in lattice parameters and thermal expansion coefficients between the substrate and the nitride overlayers, as well as between nitride layers with various alloy compositions [5].

The optical properties of quantum dot structures are influenced by strain, in particular the optical gain, the energy of transitions, and the average direct band gap.

In this paper, we calculate theoretically and compare the optical gain and threshold characteristics of the GaN/$Al_{0.2}Ga_{0.8}N$ quantum dot lasers, taking into account the influence of strain and side length boxes at an injected carrier density of $N_v = 3.10^{19}$ cm^{-3}.

2. Theoretical aspects

2.1. Optical gain and threshold current density

We determine the material gain of quantum dot lasers utilizing the method of Assada *et al*. [2, 9], taking into account the intraband relaxation. In general, the optical gain may be written in the form:

$$g(\omega) = \frac{\omega}{n_r}\sqrt{\frac{\mu_0}{\epsilon_0}}\sum_{lmn}\int_{E_g}^{\infty} < R_{cv}^2 > \times \frac{g_{cv}(f_c - f_v)\frac{\hbar}{\tau_{in}}}{(E_{cv} - \hbar\omega)^2 + (\frac{\hbar}{\tau_{in}})^2} dE_{cv}. \quad (1)$$

The conduction band (or heavy-hole band) is designated by the subscript c (or v), while f_c and f_v are the corresponding Fermi functions of the conduction and valence band states, respectively, R_{cv} is the dipole moment, E_{cv} is a transition energy between the conduction band and valence band,

ω is the angular frequency of light, ϵ_0, μ_0 and n_r are the dielectric constant, vacuum permeability and refractive index. The intra-band relaxation time τ_{in} is assumed to be 0.1 ps.

g_{cv} is the density of states for the quantum dot, given by [2]:

$$g_{cv}(E_{cv}) = \frac{2\delta(E_{cv} - E_{cnml} - E_{vnml} - E_g)}{L_x L_y L_z}, \quad (2)$$

where E_{cnml} and E_{vnml} represent the quantized electron and hole energy levels respectively of a quantum box structure in the x, y and z directions, and $\delta(E)$ is the delta function [10]. Energy levels are given by the following equation if we assume a structure that comprises of a quantum box in the form of a cubic with dimensions of L_x, L_y and L_z [11].

$$E_{cnml} = \frac{\hbar^2}{2m_c^*}\left(\left[\frac{n\pi}{L_x}\right]^2 + \left[\frac{m\pi}{L_y}\right]^2 + \left[\frac{l\pi}{L_z}\right]^2\right), \quad (3a)$$

$$E_{vnml} = \frac{\hbar^2}{2m_v^*}\left(\left[\frac{n\pi}{L_x}\right]^2 + \left[\frac{m\pi}{L_y}\right]^2 + \left[\frac{l\pi}{L_z}\right]^2\right), \quad (3b)$$

where the effective masses of an electron and a hole are $m_c^* =$ and m_v^*, respectively, while the labels of the quantized energy levels in the box are n, m and l.

In Eq. (1), the electron and hole in the quantum box are assumed to be in equilibrium, as determined by the quasi-Fermi levels E_{fc} and E_{fv}.

It is been assumed that the transition from the first conduction band to the first valence band (heavy hole band) is made because the density of states in the light hole band is lower than that of the heavy hole band, and its probability of occurrence is greater than that of the other transitions.

The modal gain is another main parameter characteristic of lasing action. To calculate it, multiply the optical gain by the confinement factor. The lasing action occurs when the modal gain exceeds the total loss [9, 12].

It is written as $g_m = \Gamma.g$, where Γ is the optical confinement factor.

The threshold current density is written as [2, 13, 14]:

$$J_{th} = \frac{k\eta q L_z N_{th}}{\tau_s}, \quad (4)$$

where q indicates electron charge, η is the rate of quantum box surface area included in the total area, k defines the number of layers in the quantum dot array, and τ_s represents carrier life time.

The threshold carrier density N_{th} is given as follow [15]:

$$N_{th} = N_{tr} + \frac{1}{\Gamma g_d}\left(\alpha_i + \frac{1}{2L_c}\ln\left[\frac{1}{R}\right]\right), \quad (5)$$

where internal loss is α_i, cavity length and reflectivity are denoted by L_c and R, respectively, differential gain is g_d, and N_{tr} represents transparency carrier density.

2.2. Effects of strain

Consider a layer of wurtzite crystal of GaN grown along the c axis (z-axis) on a thick $Al_xGa_{1-x}N$ layer with a compressive or tensile strain. The strain effects are calculated in the following manner. First, the strain in the plane ϵ_{xx} of the epitaxial growth assumed to be positive for tension and negative for compression is [16-19]:

$$\epsilon_{xx} = \epsilon_{yy} = \frac{a_0 - a}{a}, \quad (6)$$

where a_0 and a are the lattice constants of the $Al_xGa_{1-x}N$ barrier and the GaN dot layers, respectively.

The strain in the perpendicular direction can be expressed as:

$$\epsilon_{zz} = -\frac{2C_{13}}{C_{33}}.\epsilon_{xx}, \quad (7)$$

with $\epsilon_{xy} = \epsilon_{yz} = \epsilon_{zx} = 0$, where C_{13} and C_{33} are the stiffness constants of the GaN dots (well) layer.

It is widely known that the primary distinction between III-nitride wurtzite-type and other direct band gap semiconductors is that the conduction band does not degenerate at the Γ point. However, the valence band is split into three sub-bands: heavy hole (hh), light hole (lh), and crystal field split-off band (ch) [20].

The strain induced an energy shift in the conduction and the three valence bands at the Γ point [5]:

$$\delta E_c = a_{cz}.\epsilon_{zz} + a_{ct}.(\epsilon_{xx} + \epsilon_{yy}), \quad (8a)$$

$$\delta E_{hh/lh} = (D_1 + D_3).\epsilon_{zz} + (D_2 + D_4).(\epsilon_{xx} + \epsilon_{yy}), \quad (8b)$$

$$\delta E_{ch} = D_1.\epsilon_{zz} + D_2.(\epsilon_{xx} + \epsilon_{yy}), \quad (8c)$$

where, the strain tensor component is ϵ_{kl} and the conduction-band deformation potentials along the x axis and perpendicular to the c axis are a_{cz} and a_{ct} respectively. $Dj(j = 1, ...4)$ is the potential deformation.

Following the convention for the wurtzite structure, we note that the energy origin is selected at the maximum of the unstrained valence band.

3. Results and discussions

We suppose the quantum dot structure under analysis contains a GaN active layer with L side length of ($L = L_x = L_y = L_z$) sandwiched by $Al_xGa_{1-x}N$ barriers. Taking into account the strain effect, we compute quantum dot quantized energy levels for conduction and valence bands, as well as strain band-gap energy, which are then used to determine optical gain and threshold current density in the model stated above. Table I summarizes the values of the various physical parameters utilized in the calculation.

In Fig. 1, at an injected carrier density of $N_v = 3.10^{19}$ cm^{-3}, the optical gain is presented as a function of the transition energy for various side lengths of a cubic quantum box ($L = 60, 80, 100$ Å) for compressive strain, unstrained, and tensile strain structures, respectively. It is intriguing to

TABLE I. The parameters used in the calculations. (m_0 is the free electron mass) [5,17,19,21].

	GaN	AlN
Energy parameters (eV)		
Eg at 300 K	3.43	6.2
Δ_1 (eV)	0.01	-0.0227
Δ_2 = Δ_3 (eV)	0.00567	0.012
Effective masses		
m_e	0.2 m_0	0.3 m_0
m_{hh}	0.8 m_0	1.14 m_0
refractive index n_r	2.67	2.03
Deformation potentials (eV)		
a_{cz}	4.6	4.5
a_{ct}	4.6	4.5
D_1	-3.7	-17.1
D_2	4.5	7.9
D_3	8.2	8.8
D_4	-4.1	-3.9
Elastic stiffness constants (GPa)		
C_{13}	106	108
C_{33}	398	373

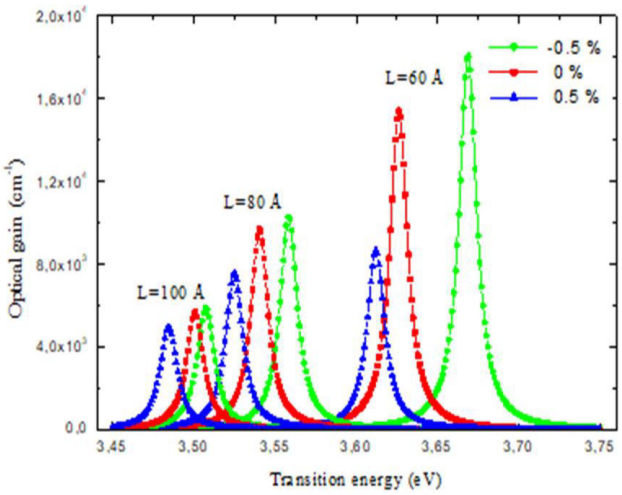

FIGURE 1. Optical gain spectra for GaN/$Al_{0.2}Ga_{0.8}N$ quantum dot lasers with -0.5% compressive strain, unstrained and 0.5% tensile strain for various sizes of quantum box at $N_v = 3.10^{19}$ cm^{-3}.

observe a significant increase in optical gain for compressive strain GaN quantum dots compared to unstrained and tensile strain GaN quantum dots, because compressive strain raises the average direct band-gap and makes it easier to populate inversions for given carrier densities.

It is also noted that optical gain values decrease with increasing box sizes. Due to the increase in carrier density for population inversion in small-sized quantum boxes, the optical gain is higher in both cases for a small-sized box with $L = 60$ Å.

On the other hand, when the quantum dot's size becomes larger, the carriers in the box are dispersed throughout useless levels, and the separation between energy levels is insufficient to achieve a high gain.

The variation of optical gain as a function of the transition energy under a compressive strained and a tensile strained for different magnitudes $|\epsilon_{xx}| = 0.25$, 0.5 and 0.75% are presented in Fig. 2, where we observe that the compressive strain presents a higher optical gain with similar values for the three cases $(-0.25, -0.5, -0.75\%)$ compared to that of tensile strain. It can also be seen that, in the case of tensile strain, the value of optical gain increases as the magnitude $|\epsilon_{xx}|$ decreases.

Table II summarizes the maximum optical gain values and the peak photon energy obtained from Fig. 2 for an injected carrier density $N_v = 3.10^{19}$ cm^{-3} at $L = 60$ Å.

Figure 3 shows a comparison of peak optical gain as a function of carrier density for compressive strain, unstrained and tensile strain structures with varied quantum box sizes. This diagram contains two zones (on the positive side) as well as absorption (negative side). We can observe that the optical gain increases rapidly as carrier density increases above N_{tr}, the point at which the material begins to amplify the photon whose energy fulfills the Bernard-Duraffourg conduction ($E_g < h\nu < E_{fc}$ - E_{fv}) for each box size (where $h\nu$ represents photon energy).

The gain coefficient of a smaller sized quantum dot has a higher transparent carrier density value, than that of a larger sized quantum dot. In comparison to the other two structures,

TABLE II. Comparative table of value of the maximum gain and peak transition energy for GaN/$Al_xGa_{1-x}N$ compressive and tensile strain.

$L = 60$ Å	**Compressive strain**	**Tensile strain**
	-0.25% -0.5% -0.75%	0.25% 0.5% 0.75%
Gain max (cm^{-1})	17198 18074 18370	12505 8780 5092
Transition energy (eV)	3.665 3.668 3.67	3.615 3.611 3.609

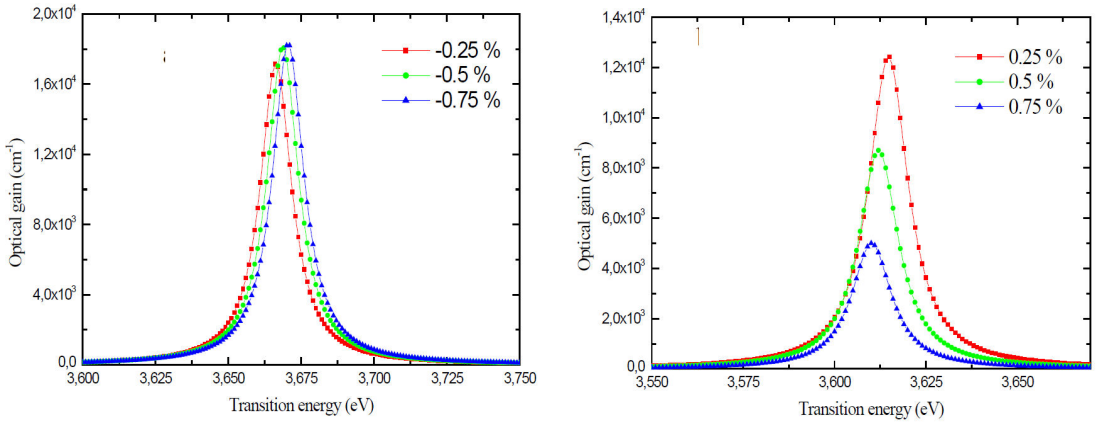

FIGURE 2. Optical gain spectra for a strained GaN/$Al_xGa_{1-x}N$ ($|\epsilon_{xx}| = 0.25$, 0.5 and 0.75%) quantum dot lasers at $L = 60$ Å, $N_v = 3.10^{19}$ cm^{-3}: a) compressive strain, b) tensile strain.

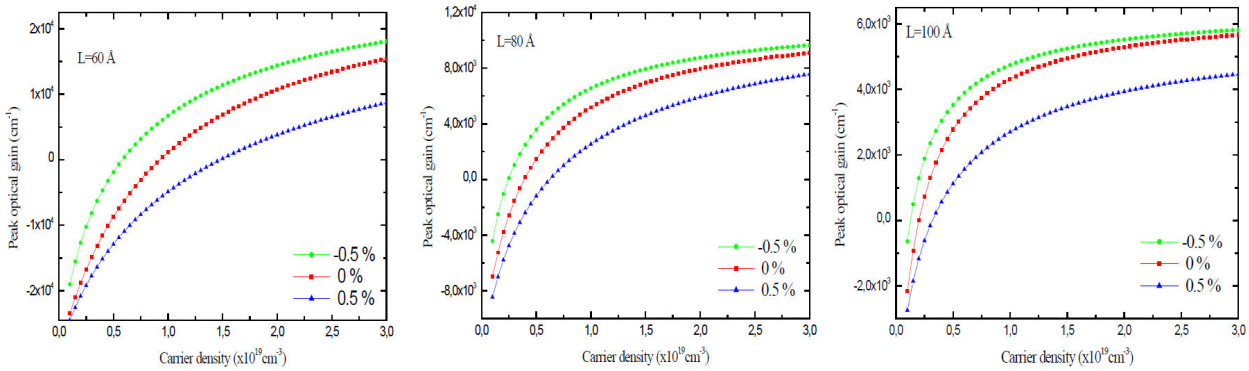

FIGURE 3. Peak optical gain as a function of carrier density for a GaN/$Al_{0.2}Ga_{0.8}N$ quantum dot laser with -0.5% compressive strain, unstrained and 0.5% tensile strain for various sizes of quantum box.

we can see that the compressively strained quantum dot laser has a lower transparent carrier density. On the other hand, while having the biggest differential gain, the tensile strained quantum dot laser has the highest transparent carrier density. Figure 4 shows the relationship between peak modal gain and current density values for three distinct quantum box sizes with: compressive strain, unstrained and tensile strain structures. This curve is significant because it depicts the relationship between the three primary parameters: gain modal, current density and side of quantum box length, and enables quick comparison of various quantum dots.

It is apparent from this figure that the modal gain increases as current density increases and remains almost constant at higher values of current density.

We also notice that as the side length of the quantum box increases, the transparency current density J_{tr} (intercept at gain = 0) decreases. At this value, the active layer cannot absorb nor amplify the light of the lasing wavelength. Furthermore, when compared to the other two structures, the tensile strained quantum dot laser has the highest transparent current density, while the compressively strained structure has the lowest.

To reach laser oscillation, it is necessary that the modal gain must be equal the total losses α_{total}. The laser oscillation condition is given as [22–26]:

$$G_{\text{mod}} = \Gamma g_{th} = \alpha_i + \frac{1}{2L_c} \ln\left(\frac{1}{R}\right) = \alpha_{total}. \qquad (9)$$

In Fig 5, we show how threshold current density varies with inverse cavity length for the three GaN/$Al_{0.2}Ga_{0.8}N$ quantum dot lasers: compressive strain, unstrained, and tensile strain at $L = 100$ Å and $N_v = 3.10^{19}$ cm^{-3}. Assuming that $\alpha_i = 5$ cm^{-1}, $R = 0.3$, $n = 1$, $L_{c1} = 2.4$ mm and

TABLE III. Performance characteristics of GaN/$Al_{0.2}Ga_{0.8}N$ quantum dot structures for various sizes of cubic boxes of -0.5% compressive strain, unstrained and 0.5% tensile strain at $N_v = 3.10^{19}$ cm^{-3}.

	Compressive strain	**unstrained**	**Tensile strain**
Side length (Å)	60 80 100	60 80 100	60 80 100
Gain max (cm^{-1})	18421 10362 5921	15415 9688 5666	9079 7697 5053
Transition energy (eV)	3.669 3.56 3.507	3.626 3.54 3.501	3.612 3.525 3.48
Peak wavelenght (nm)	338 348 353	342 350 354	343 352 356
Emission spectrum	UV UV UV	UV UV UV	UV UV UV
$N_{tr}(10^{19}$ cm$^{-3})$	0.58 0.25 0.13	0.926 0.39 0.2	1.48 0.63 0.32
Transparency current J_{tr} (A/cm^2)	78.06 41.13 26.9	148.37 69.6 33.4	163.37 88.58 57.24
J_{th} (A/cm^2) $\alpha_{T1} = 7.5$	137.06 100.6 78.87	240.5 183 127	320 208 194
$\alpha_{T2} = 10$	173 138.8 121.56	295.8 242 203	413 280.7 337.8

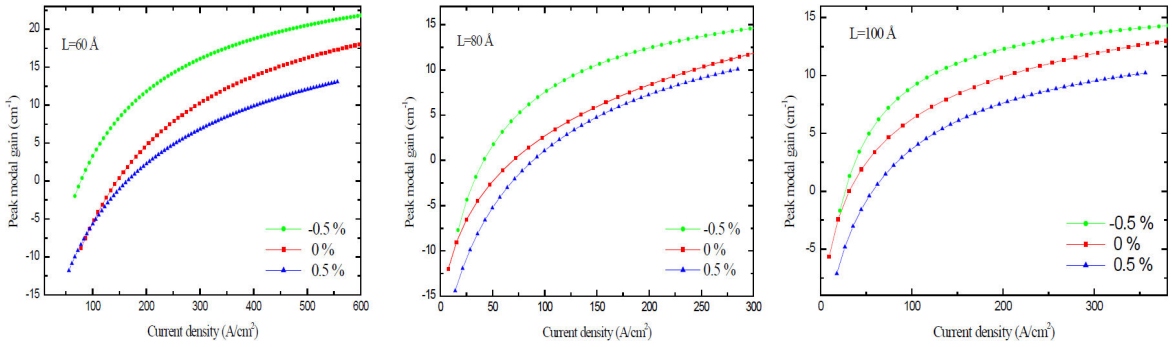

FIGURE 4. Peak modal gain for GaN/$Al_{0.2}Ga_{0.8}N$ quantum box as a function of current density, at $N_v = 3.10^{19}$ cm^{-3}, for various box sizes for -0.5% compressive strain, unstrained, and 0.5% tensile strain.

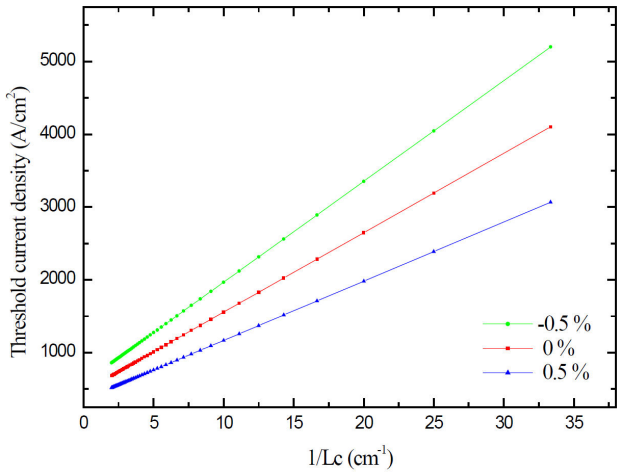

FIGURE 5. Threshold current density versus reciprocal cavity length for GaN/$Al_{0.2}Ga_{0.8}N$ QD structure of -0.5% compressive strain, unstrained and 0.5% tensile strain at $L = 100$ Å and $N_v = 3.10^{19}$ cm^{-3}.

$L_{c2} = 4.8$ mm. As can be seen from the graph, the threshold current density rises as the reciprocal cavity length grows due to a corresponding increase in mirror loss. As a result, a long cavity length is required to obtain a low threshold current density.

Table III shows a summary of the findings from this study.

Depending on the above results and Table III, we can deduce that:

- The value of optical gain increases as the quantum dot laser size reduces. On the other hand, the value of the threshold current decreases as the size of the box increases.
- Compressively strained quantum dot lasers are more effective as a result of increased optical gain, while tensile strained has a smaller impact.
- In comparison to the unstrained and tensile strained structures, the compressively strained quantum dot laser has a lower transparent carrier density (N_{tr}) and transparency current density (J_{tr}). While the tensile straine has the highest transparent carrier density and transparency current density (for the same size), what is important is the threshold current density that can be defined by the total losses due to the facet transmission and to the intrinsic absorption. For example, we can see that the compressively strained quantum dot laser, for a smaller threshold gain $\Gamma g_{th1} = \alpha_{T1} = 7.5$ cm^{-1} (long cavity length), will get a lower threshold current density indicated by the intersection between

the threshold gain line and the curve of peak modal gain as a function of current density.

- The quantum box's optimal size for the minimum threshold is shifted to a longer length of the side because low gain can be attained without carrier injection for the ineffective levels. Which means that the compressively strained quantum dot is the optimal structure with $L = 100$ Å, a gain of 5921 cm^{-1} and a minimum threshold current density of 78.87 A/cm^2 for a cavity length of $L_c = 4.8$ mm.

4. Conclusion

In conclusion, we have presented the background theory for the calculation of the material gain and threshold current density for GaN/$Al_{0.2}Ga_{0.8}$N quantum dot lasers. We also studied the impact of quantum dot strain and size on its performance. The peak modal gain has been plotted as a function of current density with the influence of strain and various quantum box sizes, as well as the threshold current density with reciprocal cavity length. It is found that adequately compressive strain improves the optical gain, and reduces the threshold current. For a larger cavity length, a quantum dot with a compressive strain has the minimum J_{th}. So, better performance can be achieved with a compressively strained GaN/$Al_{0.2}Ga_{0.8}$N quantum dot laser with $L = 100$ Å and a long cavity length compared to unstrained and tensile strain structures.

Acknowledgments

This research was supported by the Algerian General Directorate for Scientific Research and Technological Development (DGRSDT). https://www.mesrs.dz/en/dgrsdt.

1. D. Bimberg, M. Grundmann and N.N. Ledentsov, *Quantum dot Heterostructures*, (Wiley: New York, USA 1999).
2. M. Asada, Y. Miyamoto and Y. Suematsu, Gain and the threshold of three-dimensional quantum-box lasers, *IEEE J. Quantum Electron.* **22** (1986) 1915, https://doi.org/10.1109/JQE.1986.1073149.
3. Y. Arakawa and H. Sasaki, Multidimensional quantum well laser and temperature dependence of its threshold current, *App. Phys. Lett.* **40** (1982) 939, httpss://doi.org/10.1063/1.92959.
4. K. Vahala, Quantum box fabrication tolerance and size limits in semiconductor and their effect on optical gain, *IEEE J. Quantum Electron.* **24** (1988) 523, https://doi.org/10.1109/3.157.
5. Q . Yan, P. Rinke, M. Scheffler and C.G. Van de Walle, Strain effects in group-III nitrides: Deformation potentials for AlN, GaN, and InN, *App. Phys. Lett.* **95** (2009) 121111, httpss://doi.org/10.1063/1.3236533.
6. M. Miyamura, K. Tachibana and Y. Arakawa, UV photoluminescence from size-controlled GaN quantum dots grown by MOCVD, *Phys. Stat. Sol. (a)* **192** (2002) 33, https://doi.org/10.1002/1521-396X(200207)192:13.0.CO;2-C.
7. K.H. Al-Mossawi, ZnSe/ZnS quantum-dot semiconductor optical amplifiers, *Opt Photonics J.* **1** (2011) **65**, https://doi.org/10.4236/opj.2011.12010.
8. S. Nakamura, InGaN/GaN/AlGaN-Based laser diodes with modulation-doped strained-layer superlattices, *Jpn. J. Appl. Phys.* **36** (1997) L1568,httpss://doi.org/10.1143/JJAP.36.L1568.
9. H. Bouchenafa, B. Benichou, and B. Bouabdallah, Performance characteristics of GaN/$Al_{0.2}Ga_{0.8}$N quantum dot laser at $L = 100$ Å, *Rev. Mex. Fis.* **65** (2019) 38.
10. E.O. Chukwuocha and M.C. Onyeaju, Effect of Quantum Confinement on The wavelength of CdSe, ZnS and GaAs quantum dots (Qds), *Int. J. Scientific. Technol. Res.* **1** (2012) 21-24.
11. P . Harrison,: Quantum Wells, Wires and Dots, 2nd ed. (John Wiley and Sons 2005), pp. 243-270.
12. H. Bouchenafa, B. Bouabdallah and B. Benichou, Promising features of $In_{0.5}Ga_{0.5}N/Al_{0.2}Ga_{0.8}N$ quantum dot lasers, *Turk. J. Phys.* **41** (2017) 143, https://doi.org/10.3906./fiz-1610-28.
13. M. Sugawara: Self Assembled InGaAs/GaAs Quantum dots, 1st ed. (Academic Press), (1999) pp. 246-247.
14. D.G. Deppe, K. Shavritranuruk, G. Ozgur, H. Chen and S. Freinsem, Quantum dot laser diode with low threshold and low internal loss, *Electron. Lett.* **45** (2009) 54, https://doi.org/10.1049/el:20092873.
15. M. Toshihko, Analytical formulas for the optical gain of quantum wells, *IEEE J. Quantum Electron.* **32** (1996) 493, https://doi.org/10.1109/3.485401.
16. J. Minch, S.H. Park, T. Keating and S.L. Chuang, Theory and experiment of $In_{1-x}Ga_xAs_yP_{1-y}$ and $In_{1-x-y}Ga_xAl_yAs$ long-wavelength strained quantum well lasers, *IEEE J. Quantum Electron.* **35** (1999) 1, https://doi.org/10.1109/3.760325.
17. S.L. Chuang and Senior Member, Optical gain of strained wurtzite GaN quantum well lasers, *IEEE J. Quantum Electron.* **32** (1996) 1791, https://doi.org/10.1109/3.538786.
18. D. Ahn and S-H. Park, On the theory of optical gain of strained-layer hexagonal and cubic GaN quantum-well lasers, *Jpn. J. App. Phys.* **35** (1996) 6079-6083.
19. H. Zhao, R.A. Arif, Y.K. Ee and N. Tansu, Optical gain analysis of strain-compensated InGaN-AlGaN quantum well active regions for lasers emitting at 420-500 nm, *Opt Quant Electron* **40** (2008) 301, https://doi.org/10.1007/s11082-007-9177-2.

20. H. El Ghazi, A. Jorio and I. Zokrani, Recombinaison energy in (In,Ga)N/GaN strained quantum well, *Afr. Rev. Phys.* **7** (2012) 237.

21. C. Himwas: III Nitride nanostructures for UV emitter, University of Grenoble Alpes, (2015).

22. V.B. Yekta and H. Kaatuzian, Simulation and temperature characteristics improvement of 1.3 μm AlGaInAs multiple quantum well laser, *Int. J. Opt. and Applications.* **4** (2014) 46, https://doi.org/10.5923/j.optics.20140402.04.

23. S. Park, W. Jeong, H. Kim and B. Choe, Optimization of threshold current density for compressive strained InGaAs/GaAs quantum well lasers, *Jpn. J. App. Phys.* **32** (1993) 5584, httpss://doi.org/10.1143/JJAP.32.5584.

24. G.L. Su, T. Frost, P. Bhattacharya, J.M. Dallesasse, and S.L. Chuang, Detailed model for the $In_{0.18}Ga_{0.82}N$/GaN self-assembled quantum dot active material for $\lambda = 420$ nm emission, *Optics express.* **22** (2014) 22716, https://doi.org/10.1364/OE.22.022716.

25. M. Sharma, R. Yadav, P. Lal, F. Rahman and P.A. Alvi, Modal gain characteristics of step SCH InGaP/GaAs MQW based nanoscale heterostructures, *Advances in Microelectronic Engineering (AIME)* **2** (2014) 27.

26. T.Z. Al Tayyar and J.M. Sahan, Design and analysis of quantum dot laser diode for communication applications, *IJORT.* **3** (2014) 94-100.